International Microsurgery Journal

ORIGINAL

Neurohistological Evaluation of Sensory Nerve Regeneration in Canine Fasciocutaneous Free Flaps: Outcomes of Microsurgical Neurorrhaphy and Implications for Extremity Trauma Management

Vladimir Shur, MD, PhD, FAAOS

Department of Orthopedic Surgery, Icahn School of Medicine at Mount Sinai, New York, NY, USA

ABSTRACT

Objective: Traditionally, free fasciocutaneous flaps with repaired sensory nerves (neurocutaneous flaps) have been used to cover sites with high functional demands. The effectiveness of repairing nerves in these flaps to provide protective sensation remains controversial. Our in vivo experiment aimed to elucidate the rationale behind sensorial neurorrhaphy in these flaps.

Methods: We studied the nerve fiber histology in 19 canine saphenous fasciocutaneous free flaps that were reimplanted and microsurgically reinnervated at 3, 6, and 12 months postoperatively. We used micromorphometry on histology microsamples prepared with Weigert-Pal method technology to evaluate the quality and quantity of myelinated sheaths at saphenous nerve repair sites 5 mm above and below the neurorrhaphy. Additionally, the Bielschowsky-Gros method was used to track nerve fiber recovery in the distal marginal skin of these flaps.

Results: Three months postoperatively, histological analysis showed predominant nerve fiber breakdown below the saphenous neurorrhaphy site. The highest rate of nerve fiber recovery was observed at 6 months, followed by a significant reduction in the number of myelinated sheaths in the repaired saphenous nerve at 12 months, with a predominance of thick (fast) sheaths below the neurorrhaphy site ($p < 0.05$). Findings from both Weigert-Pal method and Bielschowsky-Gros method, including viable skin receptors at 12 months, indicated successful reinnervation of the flaps through the repaired sensory nerves.

Conclusion: The neurohistology data from canine saphenous neurocutaneous free flaps support the use of sensory neurorrhaphy and contribute to the body of evidence that may either support or challenge the effectiveness of neurorrhaphy as a method for nerve fiber integration into the skin of free fasciocutaneous flaps.

INTRODUCTION

Challenges in Trauma Management

The management of major extremity trauma, exacerbated by increasing numbers of wounded warriors and civilian casualties, is becoming increasingly complex [1–3]. Injuries from high-velocity objects and blasts often result in poorly vascularized soft tissue defects. Such cases frequently require the expertise of a multispecialty team trained in microsurgery [4–7]. Consequently, free vascularized tissue transfers are primarily reserved for extreme clinical situations where simpler and less labor-intensive methods are inadequate for soft tissue coverage [8–15].

Flap Classification and Neurorrhaphy

Fasciocutaneous flaps are categorized by pedicle anatomy into axial and random types, by skin mobility into mobile and non-mobile, and by the presence of a sensory nerve [16–19]. When a sensory nerve is microsurgically repaired in a free neurocutaneous flap, it is termed reinnervated [20,21]. These flaps are typically indicated when adequate soft tissue coverage and protective sensation cannot be achieved by other methods. However, controversy exists over the necessity of repairing the sensory nerve in fasciocutaneous flaps, as opposed to relying on adequate protective sensation reports without neurorrhaphy [22,23].

Neurohistological Evaluation in Reinnervated Flaps

Our in vivo experimental study, initiated in September 1983, aimed to provide neurohistological data on reinnervated free fasciocutaneous flaps. At the time, there was a lack of experimental neurohistology data in the microsurgical research literature. Remarkably, such data is still unsupported in current English-speaking world literature. The goal of this study is to enrich the understanding of neurorrhaphy through neurohistological analysis of microsurgically transferred free neurocutaneous flaps, thereby inspiring further research in this field.

MATERIALS AND METHODS

Study Background

Among the various flaps described in laboratory animals, the microsurgical replantation of a canine saphenous neurocutaneous free flap was chosen as the experimental model for our neurohistology research project [24,25]. The decision to use this flap was influenced by the presence of a reliable, well-developed axial pattern neurovascular pedicle and its classification as a mobile type of fasciocutaneous flap, characterized by a mobile skin feature with a thin fascial layer underneath. These attributes made it suitable for a reproducible experimental ipsilateral transfer (replantation).

This research was part of a four-year multidisciplinary study (from September 1983 to September 1987) at the microsurgical laboratory of Yaroslavl State Medical University. The study involved 57 canine saphenous free flaps and covered microsurgical techniques, neuroanatomy, soft tissue histology, vascular adaptations, and skin physiology. It

Table 1. Temporal Distribution of Histological Samples from Reinnervated Saphenous Fasciocutaneous Free Flaps

Tissue samples	Histochemical analysis methods	Number of samples at 3 months	Number of samples at 6 months	Number of samples at 12 months
Nerve fibers in marginal skin	BGM	7	6	6
Myelinated fibers in the saphenous nerve	WPM	7	6	6

Abbreviations: BGM, Bielschowsky-Gross method; WPM, Weigert-Pal method.

commenced at a time when the country's medical centers were overwhelmed by industrial injuries and casualties from the Soviet-Afghan war, with soft tissue defects at functionally demanding anatomical sites leading to permanent disabilities among the nation's most productive workforce. Concurrently, reconstructive microsurgery was gaining global popularity, with fasciocutaneous free flaps increasingly chosen for the majority of patients. This period also saw debates over the necessity of sensory microneurorrhaphy for protective sensation in flaps, which became a significant focus in the field of microsurgery.

Experimental Grouping and Allocation

The objective to differentiate between innervated and non-innervated free flaps in clinical practice prompted the development of our experimental study. The project was structured to include 30 free flaps, allocated into three postoperative follow-up groups at 3 months, 6 months, and 12 months. Each group consisted of 10 flaps.

It was unanimously agreed that studying nerve fiber regeneration before 3 months post-surgery was not valuable, as the nerve tissue regeneration process is typically overshadowed by resorption during this period. Additionally, it was determined that limiting the duration of neurohistological follow-up to 12 months would suffice to assess the success or failure of sensory nerve fiber regeneration at microneurography sites.

Initially, 30 canine saphenous flaps were selected for our neurohistology microsurgical research. However, only 19 flaps were ultimately included in the study. The exclusion of 11 flaps was due to surgical site complications, leaving only those that healed by primary intention for inclusion in the study groups (Table 1).

Ethical Animal Management and Surgical Protocols

All animal care and surgical procedures adhered to the state-regulated animal facility guidelines, in compliance with the Guidelines for Care and Use of Laboratory Animals. The procedures were conducted at the medical school's Microsurgical Laboratory, which is equipped to support advanced surgical training and research.

Throughout the experimental phase, general anesthesia was administered to all subjects to ensure optimal conditions for surgical accuracy and animal welfare. Vigilant postoperative monitoring was systematically applied throughout the duration of the study to assess recovery and minimize complications. The surgical procedures were executed with precision using microsurgical instruments of the highest quality, sourced from Aesculap in Tuttlingen, Germany, renowned for their engineering excellence. Suturing involved 10-0 monofilament tapered nylon sutures provided by Ethicon, Inc., which are critical for ensuring reliable wound closure in microsurgical settings. Moreover, the surgeries utilized the Carl Zeiss M-310 surgical microscope from Hamburg, Germany, featuring a magnification range from 4x to 40x, which is essential for enhancing visibility and precision during intricate microsurgical operations. These tools and methodologies were integral to advancing the field of microsurgery, contributing to significant improvements in surgical outcomes and patient safety.

Surgical Techniques

The initial step involved the meticulous dissection of the saphenous neurovascular bundle (Figure 1A) using precise bipolar micro electrocautery (Figure 1B). Subsequently, the cranial and caudal branches of the saphenous nerve were ligated, and oval-shaped axial pattern fasciocutaneous flaps measuring 8 cm x 4 cm were raised (Figure 1C) and harvested (Figure 1D). The neurovascular pedicles of the flaps were transected sharply at 45 degrees to the blood vessels and 90 degrees to the nerve. Following this, the saphenous blood vessels were gently flushed with heparin-enriched saline.

Microanastomosis was performed, starting with the arterial ends, followed by venous end-to-end connections using 10-0 Ethicon interrupted nylon monofilament sutures (Figure 1E). After restoring arterial blood flow for 30 seconds, venous anastomosis was initiated. The saphenous nerve coaptation followed after ensuring that blood circulation within the flap was re-established. The neurorrhaphy was accomplished using four 10-0 nylon interrupted epineural sutures for each case of neurorrhaphy (Figure 1F).

During arterial microanastomosis, two additional adventitia stay sutures were placed on each arterial site (Figure 2A) to minimize arterial wall injury (Figure 2B) and enhance water sealing of the anastomosis (Figures 2C–F). Bipolar micro electrocautery was consistently used to achieve thorough hemostasis throughout the procedure.

In the conducted study, meticulous recording confirmed that the ischemic duration for the arterial supply of the free flaps consistently remained below 45 minutes, underscoring the precision and efficiency of the surgical procedures. Measurements showed the saphenous nerve exhibited a mean thickness of 2.5 ± 0.5 mm (n = 19). Similarly, the average outer diameter of the associated arteries was calculated at 2.0 ± 0.5 mm (n = 19). The dimensions of the veins were also quantified, averaging 3.0 ± 0.5 mm (n = 19). These metrics illustrate the detailed anatomical considerations in the study and reflect the rigorous standardization in the collection of morphometric data, essential for ensuring replicability and reliability in microsurgical research.

Neurohistological and Histochemical Analysis

Tissue biopsy specimens for neurohistology were collected at 3 months (7 flaps), 6 months (6 flaps), and 12 months post-operatively (6 flaps), as detailed in Table 1. The neurorrhaphy samples underwent evaluation using the Weigert-Pal method (WPM) [26,27], and the skin margins were stained for soft tissue analysis with the Bielschowsky-Gross method (BGM) [28], as outlined in Table 1. Microscopic examination of both WPM and BGM samples was conducted, and images were captured using a laboratory microscope at 70x and 280x magnifications (Figures 3A–C, 4A–F, 5A–H).

The WPM was utilized for micromorphometric analysis of the repaired saphenous nerve myelin sheaths, assessing the thickness of my-

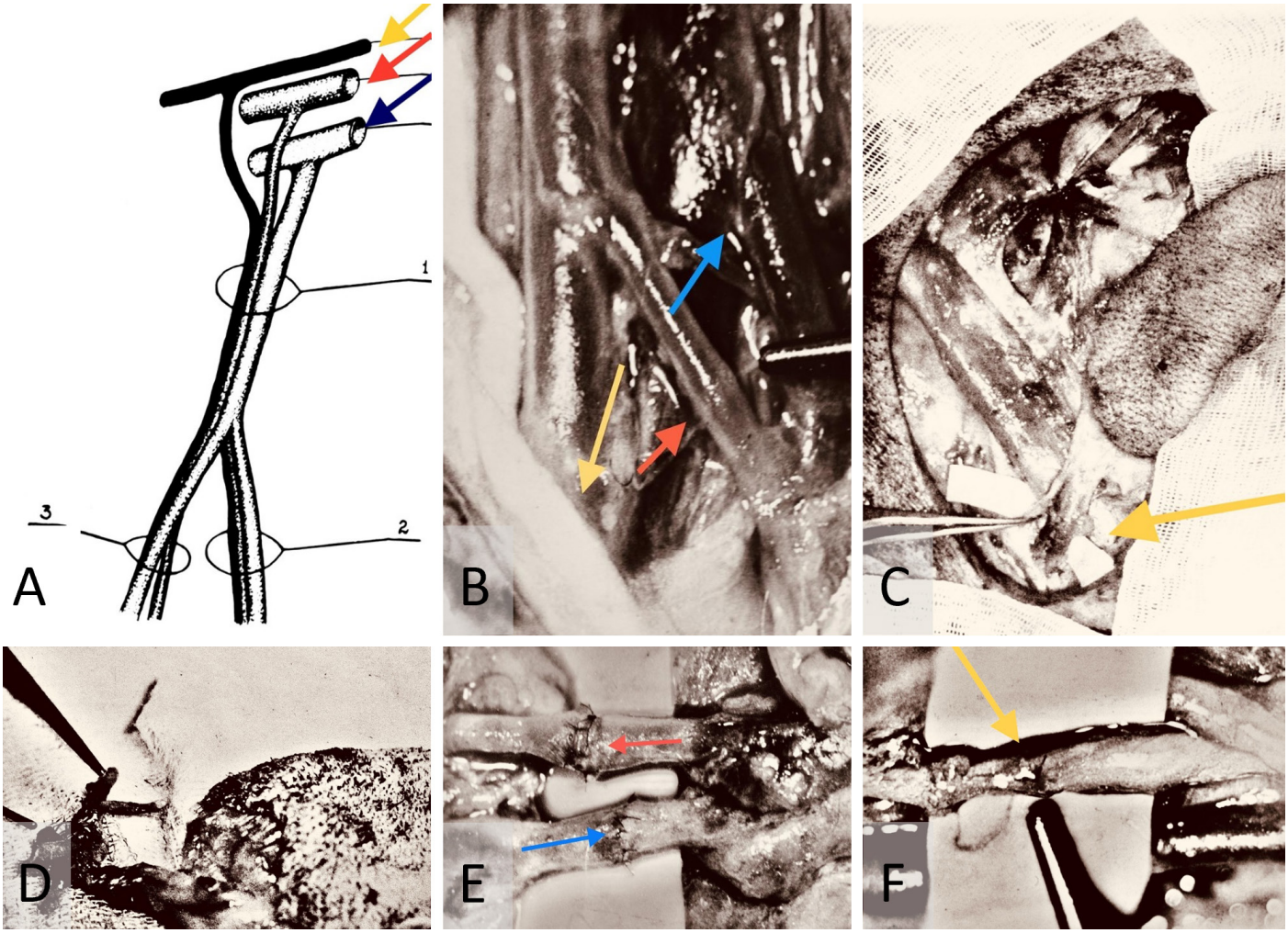

Figure 1. (A) Anatomy of the canine saphenous neurovascular bundle. It depicts the cranial trunk (1) that bifurcates into posterior and anterior caudal branches (2 and 3, respectively). It also shows the femoral nerve (yellow arrow), artery (red arrow), and vein (blue arrow). (B) Intraoperative dissection of the saphenous neurovascular bundle. This is captured with a Carl Zeiss M-310 surgical microscope camera. It highlights the saphenous nerve (yellow arrow), artery (red arrow), and vein (blue arrow). (C) Raised canine saphenous neurocutaneous flap. This image shows the flap with its dissected neurovascular pedicle (yellow arrow). (D) Preparation of canine saphenous free neurocutaneous flap. It illustrates the harvested flap ready for replantation, with vessels flushed with heparinized saline. (E) Intraoperative repair of saphenous artery and vein. This depicts the process using 10-0 nylon interrupted sutures, captured with the same microscope camera. It identifies the artery and vein by red and blue arrows, respectively. (F) Saphenous neurorrhaphy procedure. This displays the neurorrhaphy of the saphenous nerve using 10-0 epineural nylon sutures, with precise suturing highlighted by the yellow arrow.

elinated nerve sheaths—a critical marker of nerve recovery or regeneration post-surgery. This analysis was performed on 6 microsamples each from 5 mm above and below the neurorrhaphy site, resulting in a total of 228 WPM saphenous nerve microsamples from both above and below the neurorrhaphy in all 19 cases. These were subject to micromorphometry to categorize each myelinated sheath by thickness.

Additionally, the BGM was employed to assess nerve fiber integrity and distribution in the distal marginal skin of the replanted saphenous free flaps. This histochemistry technique uses silver staining to visualize nerve fibers, aiding in the evaluation of nerve integration and regeneration at distal repair sites. BGM was particularly valuable in monitoring both recovery and resorption processes in the silver-stained marginal skin nerve fibers, offering a comprehensive view of the dynamics involved in nerve repair.

Tissue Harvesting and Sample Acquisition

Tissue samples were harvested at 3, 6, and 12 months post-operatively at intervals crucial for observing different stages of neurovascular and skin tissue recovery. Specifically, 10 mm in-block biopsy samples (5 mm above and 5 mm below the neurorrhaphy) of repaired neurovascular pedicles were taken for WPM analysis, and 10 mm x 10 mm biopsy samples from the very distal marginal skin were collected for BGM analysis. These samples were carefully marked according to their proximity to the neurorrhaphy site and transported to the neurohistology laboratory for further examination (Table 1).

The distribution of flap survival varied at the different postoperative intervals, with 7 viable free flaps remaining in the 3-month follow-up group and only 6 flaps in the 6 and 12-month groups. The decision to retain an extra flap in the 3-month group was based on the understanding that this would not significantly affect the statistical outcomes of the WPM analysis but would provide an additional valuable soft tissue sample for BGM silver staining.

Statistical Analysis

The thickness of myelinated sheaths stained by the WPM was categorized and analyzed statistically. The Shapiro-Wilk test was applied to

Table 2. Quantitative Micromorphometric Analysis of Myelinated Nerve Fiber Thickness in the Saphenous Nerve Above and Below the Neurorrhaphy Site Across Defined Time Points

Assessment periods	Thin myelinated fibers (<3.9 μm)			Intermediate myelinated fibers (4.0–6.9 μm)			Thick myelinated fibers (>7.0 μm)		
	Mean ± SD	σ	p	Mean ± SD	σ	p	Mean ± SD	σ	p
6 months									
Above neurorrhaphy	372.8 ± 97.27	168.30	>0.05	162.0 ± 37.58	62.05	>0.05	577.0 ± 182.18	315.17	>0.05
Below neurorrhaphy	354.3 ± 88.59	153.26		175.0 ± 31.23	54.04		87.7 ± 15.25	26.39	
12 months									
Above neurorrhaphy	83.7 ± 18.18	31.46	<0.05	57.0 ± 4.07	7.04	<0.05	245.0 ± 67.75	117.21	<0.05
Below neurorrhaphy	22.0 ± 0.69	1.19		24.5 ± 0.71	1.2		108.0 ± 0.74	1.21	

Note: All measurements presented in this table are in micrometers (μm). This study employed micromorphometric analysis to evaluate the thickness of myelinated nerve fibers from six histological microsamples, obtained from regions located 5 mm above and below the saphenous neurorrhaphy site in each experimental group. The reported standard deviations (SD) represent variability within the collected samples. Given the impracticality of assessing the entire population, sample SDs are used as estimators of the true population standard deviation (σ). This approach facilitates the extrapolation of characteristics representative of the larger population based on the sample data.

assess the normality of the data distribution. For datasets that showed a non-normal distribution, the Mann-Whitney *U* test was employed to compare myelinated sheath thickness between two independent samples at specified time points. For datasets with a normal distribution, differences between groups were analyzed using the Student's *t*-test.

The means and standard errors were computed to represent the central tendency and variability, respectively, while standard deviation was utilized to measure the dispersion of the data. Statistical significance was established at a threshold of $p < 0.05$. These analyses were conducted using SPSS version 18.0 (SPSS, Inc., Chicago, IL, USA), ensuring the validity and reliability of our neurohistological results.

RESULTS

Early Recovery and Neurohistological Assessments

Our study examined 19 successfully replanted canine saphenous fasciocutaneous flaps, each featuring well-developed axial neurovascular pedicles and mobile skin atop a very thin fascia, classified as axial mobile neurocutaneous flaps. These flaps underwent microsurgical repair of both blood vessels and a sensory nerve.

Clinically significant cosmetic recovery at the surgical sites was documented within 3 to 6 weeks postoperatively. By six weeks, the flaps not only matched the properties of the surrounding skin but were also discernible solely by the presence of thin, oval-shaped surgical scars.

Neurohistological assessments conducted at 3 months postoperatively utilized BGM silver staining histochemistry. These assays predominantly displayed neurohistological resorption (Figure 3A). However, scattered instances of axonal recovery, including the presence of growth cones and small viable nerve fibers, were observed (Figures 3B–C).

Mid-Term Histological Findings and Myelin Analysis

At three months post-surgery, the micromorphometric results of the WPM both above and below the saphenous neurorrhaphy were difficult to interpret. The sites of myelinated sheath regeneration were obscured by the byproducts of myelin resorption (Figures 4A–B). By six months post-surgery, these resorbing myelinated sheaths were no longer present in the WPM microsamples of the saphenous nerve (Figures 4C–D).

Micromorphometric analysis of myelin at six months postoperatively revealed a predominance of thin (slow) nerve fibers (Table 2). Concurrently, the BGM silver-stained microsamples from the marginal skin revealed multiple sites of nerve fiber resorption at six months. However, the nerve regeneration process was significantly more active than at the three-month postoperative evaluation. Individual sites of nerve fibers, with remnants of resorption and predominantly recovery, were identified in the superficial skin layers at six months postoperatively (Figure 4E). Moreover, viable nerve fibers were more frequently detected in random peripheral nerve trunks within the deep layers of the free flap at six months post-surgery (Figure 4F).

Long-Term Outcomes and Statistical Relevance

At six months post-operatively, neurohistology findings showcased multiple axonal dichotomy sites (Figure 5A), accompanied by an abundance of lamellipodia (growth cones) sprouting toward the periphery of the free flaps. This presence of lamellipodia continued into the one-year post-operative study group (Figure 5F). Interestingly, no viable nerve fibers were detected within the surrounding surgical scar tissues at any follow-up point using the BGM. Instead, amputation neuromas were identified using hematoxylin-eosin stain in some samples.

Statistical significance in the WPM micromorphometry readings below the saphenous neurorrhaphy was only achieved in the one-year post-operative group (Table 2). This group was the only one with normally distributed data, as confirmed by the Shapiro-Wilk test, and showed significant results in all myelinated sheath thickness categories with $p < 0.05$. The three and six-month post-operative WPM groups did not show normal data distribution. Combined with small group sizes, this resulted in insufficient power to achieve statistically relevant values.

Moreover, comparisons made at one year post-operatively revealed a significant reduction in the numbers of thin (slow) and Intermediate thickness myelinated sheaths (Figures 5B–C). There was a dominance of more developed thick (fast) fibers in the samples above and below the saphenous neurorrhaphy site (Table 2). By one year post-operatively, the calculations below the neurorrhaphy site showed normal distribution, enabling valid statistical conclusions with $p < 0.05$ (Table 2).

In terms of BGM studies, the one-year post-operative microsamples continued to show nerve fibers' resorption (Figure 5D). These observations were accompanied by signs of adequate maturity for skin innervation histology (Figures 5E–G), including the presence of epidermal receptors (Figure 5H).

The experimental animals showed no signs of pain at the surgical

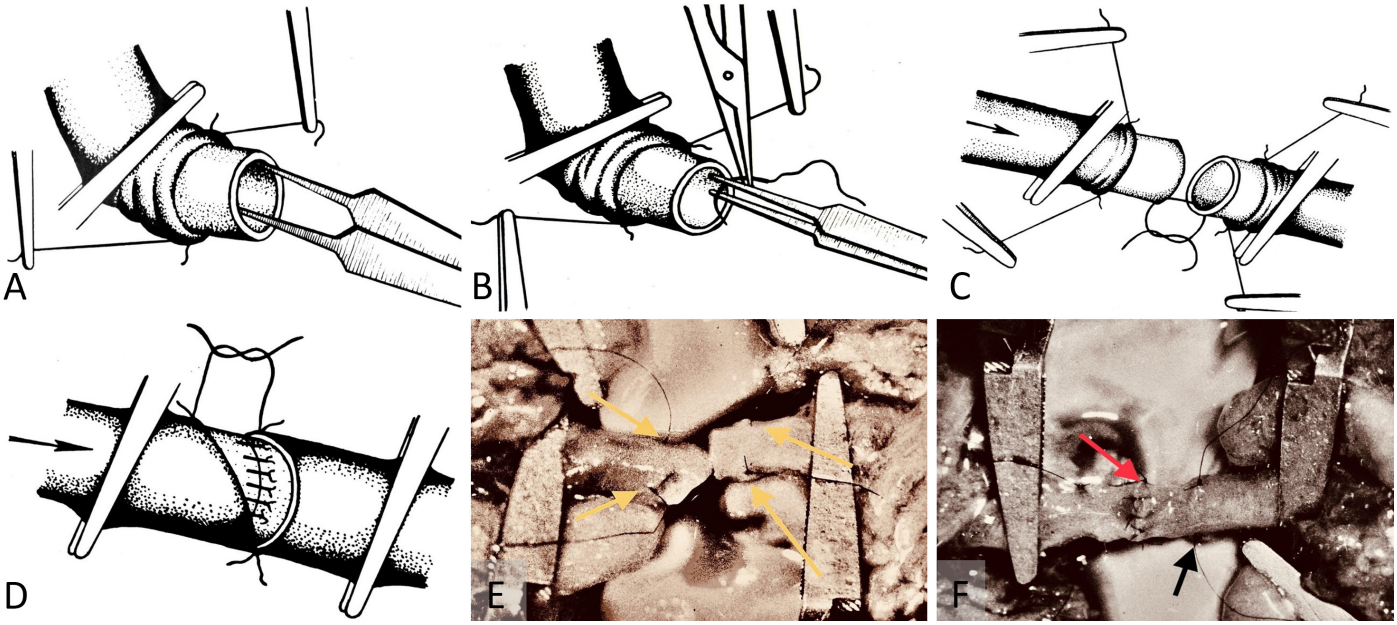

Figure 2. (A) Adventitia stay-sutures method. This technique is engineered to minimize trauma during tissue handling and improve the water-tight seal over arterial micro-anastomosis. (B) Stay-sutures for arterial adventitia. This demonstrates the use of stay-sutures to secure the micro repair site during anastomosis. It minimizes the risk of damage by avoiding direct contact with surgical instruments. (C) Adventitia stay-sutures for arterial wall handling. This illustrates the method of securing the arterial wall to reduce tissue trauma during the sawing process for microanastomosis. It facilitates a precise and less invasive connection. (D) Application of adventitia stay-sutures in arterial wall microrepair. This depicts the process of tying adventitia stay-sutures over the arterial wall during microrepair to form a protective tissue layer and enhance the water-tight seal. (E) Completed arterial microanastomosis with adventitia stay-sutures. This shows a completed microanastomosis captured with a Carl Zeiss M-310 surgical microscope camera. The 10-0 nylon adventitia stay-sutures, indicated by yellow arrows, are positioned over the repair site before final securing. (F) Arterial microanastomosis using interrupted 10-0 nylon sutures. This displays the procedure captured with a Carl Zeiss M-310 surgical microscope camera. Arterial microanastomosis is performed using interrupted sutures (red arrow). The site for adventitia stay-sutures is prepared (black arrow) to secure and seal the repair, enhancing durability and integrity.

sites after the procedure and responded to a light pinch on the replanted free flap skin one year post-operatively.

DISCUSSION

Flap Prototype and Study Protocol

The saphenous canine flap served as a prototype for an axial pattern neurocutaneous free flap with mobile skin, classified as a mobile type of fasciocutaneous flap in clinical practice. The study protocol was demanding, necessitating extensive training in microsurgery, reconstructive plastic surgery, and a thorough understanding of nerve fibers regeneration histology. The absence of a pilot prospective study for experimental fasciocutaneous free flaps neurohistology posed significant challenges in interpreting the project's results.

On the bright side, our data potentially provides a foundation for further original research into nerve fibers regeneration within both free and island fasciocutaneous flaps. Analyzing these results further, the study also sheds light on the long-term recovery and neurological outcomes, which are crucial aspects of the research that merit further attention.

Long-Term Neurological Recovery

A significant limitation of our study was the complexity of the overall project coupled with relatively small histology sample sizes. Consequently, statistically reliable *p* values from WPM saphenous nerve micromorphometry were only achieved in the final study group (one-year post-surgery below neurorrhaphy). Here, there was a notable prevalence of the most developed myelinated sheaths, observed both above and below the neurorrhaphy site (Table 2). The one-year post-operative group proved to be the most informative, offering the longest follow-up period and thus, the results from this group suggest a substantial neurological recovery below the neurorrhaphy site one year after surgery.

Furthermore, the overall reduction in myelinated fibers observed in the one-year WPM group may be attributed to an adaptation process. The dermatomal sensory requirements for the transferred free flap became less demanding than the capacity offered by the repaired saphenous nerve. This phenomenon of non-functional nerve fibers reduction is supported by findings from the BGM, which detected remnants of resorbing nerve fibers in the marginal skin up to one year post-surgery. This indicates a disposition process for the initially recovered nerve fibers that became biologically unnecessary as the flap was already adequately reinnervated. Essentially, this reflects a scenario where supply exceeds demand, suggesting that the sensory needs of the free flaps were sufficiently met sometime between six and twelve months post-operatively.

With this established neurological recovery, the next area of focus is the sensory innervation and clinical implications of microsurgical neurorrhaphy in these flaps.

Sensory Innervation and Clinical Implications

During the course of the global multidisciplinary study, the route of sensory innervation through microsurgical neurorrhaphy was highlighted by random findings of distal surgical scar amputation neuromas reported by the histology lab. However, limitations arose as photometry documentation and detailed descriptions of these hematoxylin-eosin findings were not included in the neurohistology project protocol, hence, are

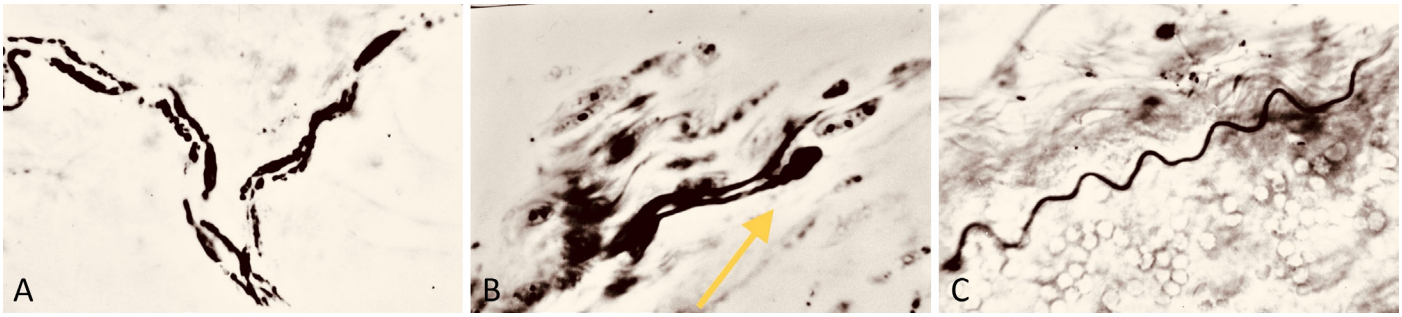

Figure 3. (A) Bielschowsky-Gros method (BGM) analysis, presenting a microphotograph taken at 280x magnification. It captures fragmented marginal skin nerve fibers three months postoperatively. The image clearly demonstrates the active resorption process, providing insights into the dynamic changes occurring in nerve fiber structure during healing. (B) BGM analysis of nerve fiber regeneration, featuring a microphotograph at 280x magnification. This image shows lamellipodia (indicated by the yellow arrow) adjacent to fragments of nerve fibers, three months postoperatively. It highlights the simultaneous occurrence of both resorption and regeneration processes in the nerve tissues. (C) BGM analysis of nerve fiber renewal, showcasing a microphotograph taken at 280x magnification. It displays a viable random nerve fiber adjacent to a skin artery three months post-surgery. The image effectively illustrates the signs of histological renewal, emphasizing the ongoing regeneration process within the nerve tissues.

unavailable for presentation. Despite this, reports of neuromas at scar sites surfaced along with indications of escalating neurological recoveries within the free flaps as early as three months post-operatively.

These findings, underscored by the absence of viable nerve fibers at surgical scar areas in any sample group, suggest a minimal potential for non-axial nerve fibers regeneration within a free fasciocutaneous flap. Furthermore, clear signs of nerve fibers regeneration in BGM skin were detected starting at three months post-operatively, consistent with distally oriented growth cones (Figures 3B, 5F), followed by axonal dichotomies at six months (Figure 5A), and the emergence of epidermal receptors by one year (Figure 5H). These observations challenge popular clinical opinions that sensory recovery in free flaps can occur without sensory nerve repair.

Our data supports the clinical benefits of cutaneous neurorrhaphy and contradicts reports suggesting that free flaps can achieve protective sensation without sensory nerve repair. The difficulties in forming conclusive statements are exacerbated by the lack of statistically significant pilot studies based on neurohistology assays. According to our findings, adequate reinnervation of the saphenous fasciocutaneous free flap likely occurs through sensorial microneurorrhaphy, evidenced by early discoveries of viable fibers below saphenous nerve repairs at three months post-operatively, increased axonal growth cones and dichotomies by six months, and a rise in myelinated sheaths in WPM samples below neurorrhaphy sites.

Long-term findings at one year post-operatively show a statistically significant prevalence of high-quality thick (fast) fibers at the flap sites ($p < 0.05$), further complemented by the development of epidermal receptors between six months to one year after surgery. These outcomes, combined with the inability of BGM to find viable nerve fibers within surgical scars in any tissue sample, can be interpreted as a favorable impact of sensorial microneurography and as weakening the widely accepted hypothesis of random sensory reinnervation in flaps.

It remains unclear how nerve fibers revival truly occurs in clinical reports of non-innervated free flaps achieving protective sensation. The protective skin sensation observed in non-innervated free flaps needs further statistical backing. Therefore, upcoming histology research should focus on whether sufficient nerve fibers can penetrate surgical scars following ingrowing blood vessels or if protective sensation in flaps relies on sensory responses at the recipient site.

Additionally, simpler micrography studies such as hematoxylin-eosin staining to detect amputation neuromas in surrounding scars could offer insights into flap sensory recoveries. These studies, along with physiological research comparing reinnervated versus non-innervated fasciocutaneous flaps, will be critical in enhancing our understanding of nerve fiber regeneration post-microneurorrhaphy.

Ultimately, the significance of neurocutaneous free flaps is undeniable, and continued exploration into improving nerve fiber regeneration after sensorial microneurorrhaphy is essential.

Study Limitations

Our multidisciplinary pilot research project on the neurohistology of fasciocutaneous free flaps with repaired sensory nerves, initiated in the 1980s, presents several limitations. Firstly, the study's small sample size limits the generalizability of the findings across broader populations and diverse clinical scenarios. This constraint may also diminish the statistical power of the conclusions, potentially obscuring subtle effects of neurorrhaphy. Additionally, the reliance on an animal model, while necessary for ethical and practical reasons, may not fully capture the complexity of human physiological responses to nerve repair, posing challenges in directly translating these findings to clinical practice.

Furthermore, the study outcomes were only evaluated up to one year post-operatively. Longer-term follow-up would be crucial to assess the durability of sensory recovery and the long-term viability of the repaired nerves. With only 19 flaps studied, expanding the study to include larger groups could provide a more detailed exploration of different surgical techniques and their specific impacts on nerve regeneration, offering a more nuanced understanding of the factors contributing to successful neurorrhaphy.

The microsurgical technique employed used a 10-0 microsuture, the smallest size available at the time, which restricted the study to epineural repairs only. Due to the size of the saphenous nerve fascicles, interfascicular neurorrhaphy was not feasible with 10-0 nylon suture. Given these limitations, the future direction for research on free flaps must be carefully planned and considered to enhance the reliability and applicability of the findings.

Future Directions in Free Flap Research

The limitations of our study underscore the necessity for further research featuring expanded sample sizes, a variety of clinical conditions, and longer monitoring periods to enhance the foundational insights already gained. Crucially, pioneering research on free flap transfers should involve a multispecialty team approach, beginning with expertise from a microsurgical lab and extending to basic science specialties.

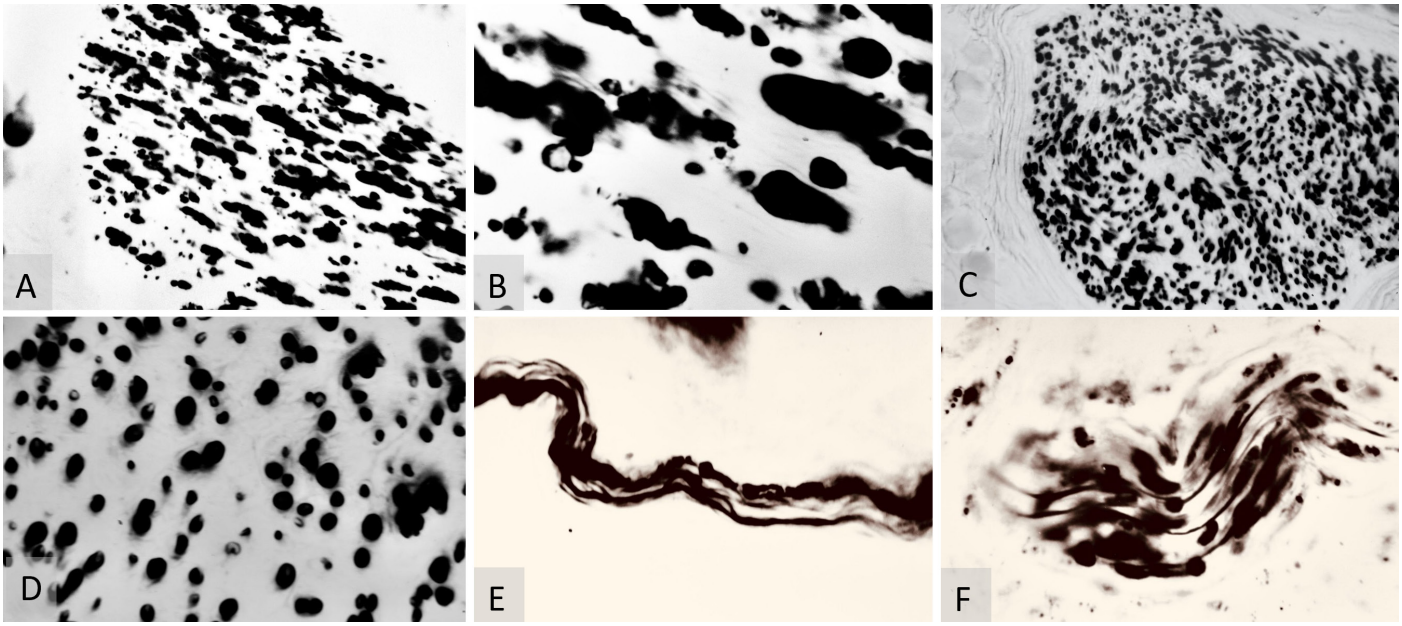

Figure 4. (A) Weigert-Pal method (WPM) analysis of saphenous nerve regeneration. This microphotograph, taken at 70x magnification, displays a cross-section of the saphenous nerve below the neurorrhaphy site, three months post-surgery. It highlights early stages of regeneration in myelinated nerve fibers and demonstrates neural recovery dynamics. (B) WPM cross-section analysis of the saphenous nerve, shown at 280x magnification. This image depicts a cross-section below the neurorrhaphy site, three months post-operatively, and clearly illustrates the regeneration of myelinated nerve fibers. (C) WPM analysis of myelinated sheaths, captured at 70x magnification. It shows the morphology of myelinated sheaths below the neurorrhaphy site, six months post-surgery, showcasing regions of sheath consolidation and providing insights into advanced stages of nerve fiber regeneration. (D) WPM analysis of myelin sheath thickness variations, at 280x magnification. This image displays a cross-section of the saphenous nerve six months post-surgery, highlighting variations in myelin sheath thickness and illustrating differential recovery patterns. (E) Bielschowsky-Gros method (BGM) analysis of nerve fibers, captured at 280x magnification six months post-surgery. It illustrates both recovered and resorbing nerve fibers, capturing dynamic changes within the nerve structure and highlighting ongoing processes of regeneration and degeneration. (F) BGM analysis of peripheral nerve recovery, taken at 280x magnification six months post-surgery. This image displays a viable peripheral nerve, vividly showing signs of nerve fiber recovery and highlighting successful regeneration.

Frequent flap failures can arise from devastating surgical site complications, such as microsurgical anastomosis thrombosis, bleeding, infections, tissue edge necrosis, and ultimate loss of the free flap. These challenges, along with the burdens related to the nature and design of our laboratory experiment, may explain the limitation of our study to only 19 free flap transfers. These selected flaps healed by primary intention and had functional microsurgical repairs, with tissue harvested no earlier than three, six, and twelve months post-operatively.

Looking ahead, it is essential to refine these techniques to improve the consistency and success rates of future free flap studies. This advancement will not only mitigate the risks of complications but also broaden the applicability and reliability of the results in clinical practice.

CONCLUSION

The experimental data from our study on mobile type neurocutaneous free flaps suggest that the repaired sensorial nerve acts as a conduit for skin innervation recoveries, with high-quality myelinated nerve fibers below the saphenous neurorrhaphy serving as a likely source of adequate skin reinnervation. These findings underscore the importance of preserving cutaneous nerves during fasciocutaneous island flap procedures to enhance sensory outcomes. Encouraging results from WPM and BGM prompt further research with larger samples of innervated and non-innervated flaps to confirm these interpretations and explore potential differences in early stages of neurological recovery, which could significantly influence the practice of sensorial neurorrhaphy for protective reinnervation in free fasciocutaneous flaps.

ACKNOWLEDGMENTS

This study was conducted as part of the author's PhD project. The author gratefully acknowledges Kirill Pshenisnov, MD, and Katharine Cintron, BS, for their review and technical assistance. Special thanks are extended to Julia Terzis, MD, Laurence Colen, MD, Ivor Kaplan, MD, John McCraw, MD, David Gilbert, MD, Andrew Burgess, MD, Andrew Eglseder, MD, and Andrew Pollak, MD, for their invaluable teaching in reconstructive microsurgery and orthopedic trauma during the author's fellowship in Microsurgery at Eastern Virginia Medical School and residency in orthopedics at the University of Maryland Medical System/Shock Trauma Center. The author also expresses deep appreciation to Scott Levin, MD, whose lifelong dedication to Orthoplasty inspired the completion of this manuscript. This research project is dedicated to the memory of the author's esteemed mentors and friends, Clifford Turin, MD, Yuri Novikov, MD, and Vladimir Minachenko, MD.

ARTICLE INFORMATION

*__Correspondence:__ Vladimir Shur, MD, PhD, FAAOS, Department of Orthopedic Surgery, Icahn School of Medicine at Mount Sinai, 1 Gustave L. Levy Place, New York, NY 10029-5674, USA. Email: Vladimir.shur@mountsinai.org

Received: Mar. 12, 2024; **Accepted:** Sep. 25, 2024; **Published:** Nov. 7, 2024

DOI: 10.24983/scitemed.imj.2024.00192

Disclosure: The research presented herein was undertaken as a component of an expansive, four-year interdisciplinary initiative, spanning from September 1983

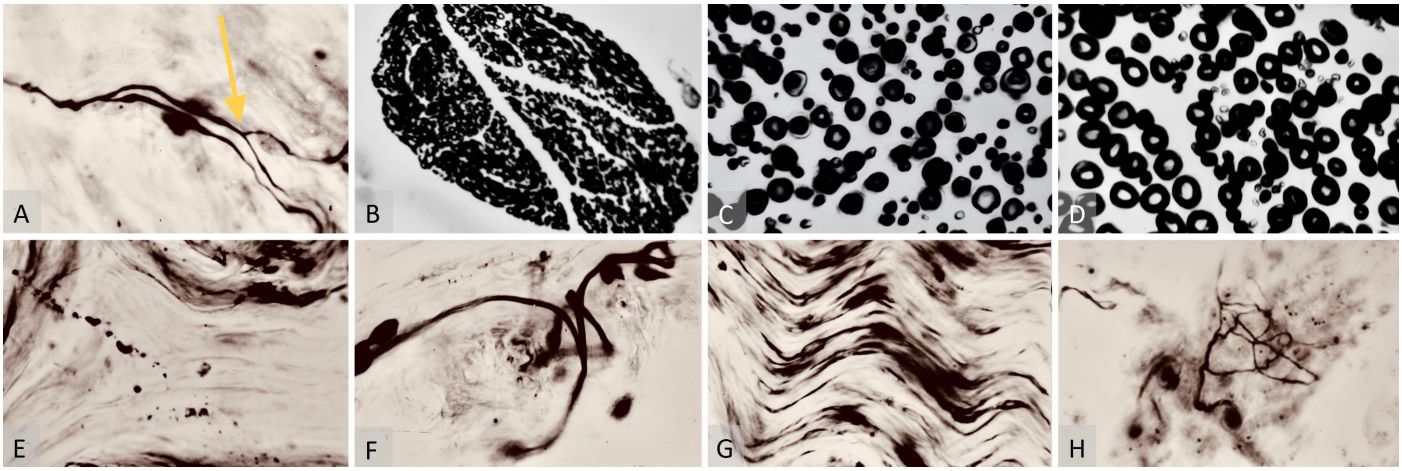

Figure 5. (A) Bielschowsky-Gros method (BGM) analysis of nerve fiber dichotomy. This microphotograph is shown at 280x magnification six months post-surgery. It highlights a nerve fiber dichotomy, indicated by the yellow arrow. This demonstrates a significant stage of maturity in neurological recovery, showcasing successful branching and complexity development within the nerve fibers. (B) Weigert-Pal method (WPM) analysis of nerve cross-section, captured at 70x magnification one year post-operation. It displays a nerve cross-section sample below the repair site. This image presents an organized structure of myelinated sheaths, indicating the final stages of the nerve regeneration process and showcasing the successful culmination of myelin sheath development and neural recovery. (C) WPM analysis of the saphenous nerve cross-section, taken at 280x magnification one year post-operation. It shows a cross-section of the saphenous nerve below the neurorrhaphy site featuring an abundance of properly structured thickly myelinated (fast-conducting) nerve fibers. This is indicative of successful sensory integration and fulfillment of sensorial requirements of the replanted flap. (D) WPM analysis of saphenous nerve cross-section above the neurorrhaphy site, captured at 280x magnification one year post-operation. It features thickly myelinated (fast-conducting) sheaths, representing the final stages of nerve regeneration at the recipient site. (E) BGM analysis of nerve fiber resorption, captured at 280x magnification one year post-surgery. It displays fragments of nerve fibers in the marginal skin of the flap. This illustrates the resorption of initially recovered but subsequently nonfunctional nerve fibers, due to the lower dermatomal sensory demands of the free flap. (F) BGM growth cone analysis, taken at 280x magnification one year post-surgery. It shows growth cones (lamellipodia) in the flap's marginal skin, indicating ongoing regeneration of skin nerve fibers and suggesting a continuous recovery process within the nerve structures. (G) BGM analysis of axial nerve regeneration, captured at 280x magnification one year post-surgery. It displays a large skin nerve structure with regenerated fibers, supporting the concept of an axial nerve regeneration route while raising questions about the feasibility of random sensory recovery in free flaps. (H) BGM analysis of sensory recovery, captured at 280x magnification one year post-surgery. It displays recovered marginal skin receptors and lamellipodia in a saphenous free flap, outlining the histological end product of sensory nerve fiber regeneration within the flap.

to September 1987, within the confines of the microsurgical laboratory at Yaroslavl State Medical University.

Ethical Compliance and Animal Welfare: This investigation was meticulously aligned with the prevailing ethical guidelines governing the humane care and use of laboratory animals during the study period from 1983 to 1987. All protocols involving animals were stringently reviewed and sanctioned by the institutional ethics committee at Yaroslavl State Medical University, ensuring adherence to the highest standards of animal welfare throughout the duration of the research.

Funding: Funding for this study was generously provided by the Yaroslavl State Medical University Research Funds over the entire course of the project.

Conflict of Interest: In accordance with the ethical standards set forth by the SciTeMed publishing group for the publication of high-quality scientific research, the author(s) of this article declare that there are no financial or other conflicts of interest that could potentially impact the integrity of the research presented. Additionally, the author(s) affirm that this work is solely the intellectual property of the author(s), and no other individuals or entities have substantially contributed to its content or findings.

Publisher Disclaimer: It is imperative to acknowledge that the opinions and statements articulated in this article are the exclusive responsibility of the author(s), and do not necessarily reflect the views or opinions of their affiliated institutions, the publishing house, editors, or other reviewers. Furthermore, the publisher does not endorse or guarantee the accuracy of any statements made by the manufacturer(s) or author(s). These disclaimers emphasize the importance of respecting the author(s)' autonomy and the ability to express their own opinions regarding the subject matter, as well as those readers should exercise their own discretion in understanding the information provided. The position of the author(s) as well as their level of expertise in the subject area must be discerned, while also exercising critical thinking skills to arrive at an independent conclusion. As such, it is essential to approach the information in this article with an open mind and a discerning outlook.

REFERENCES

1. Casey K, Sabino J, Jessie E, Martin BD, Valerio I. Flap coverage outcomes following vascular injury and repair: Chronicling a decade of severe war-related extremity trauma. *Plast Reconstr Surg* 2015;135(1):301–308.
2. Holcomb JB, Stansbury LG, Champion HR, Wade C, Bellamy RF. Understanding combat casualty care statistics. *J Trauma* 2006;60(2):397–401.
3. Burns TC, Stinner DJ, Possley DR, et al. Does the zone of injury in combat-related Type III open tibia fractures preclude the use of local soft tissue coverage? *J Orthop Trauma* 2010;24(11):697–703.
4. Heller L, Levin LS. Lower extremity microsurgical reconstruction. *Plast Reconstr Surg* 2001;108(4):1029–1041; quiz 1042.
5. Pollak AN, McCarthy ML, Burgess AR. Short-term wound complications after applica-

tion of flaps for coverage of traumatic soft-tissue defects about the tibia. The Lower Extremity Assessment Project (LEAP) Study Group. *J Bone Joint Surg Am* 2000;82(12):1681–1691.
6. Godina M. Early microsurgical reconstruction of complex trauma of the extremities. *Plast Reconstr Surg* 1986;78(3):285–292.
7. Yaremchuk MJ. *Lower Extremity Salvage and Reconstruction: Orthopedic and Plastic Surgical Management*. 1st ed. New York, NY, USA: Elsevier Science;1989.
8. Azoury SC, Kovach SJ, Levin LS. Reconstruction options for lower extremity traumatic wounds. *J Am Acad Orthop Surg* 2022;30(16):735–746.
9. Ong YS, Levin LS. Lower limb salvage in trauma. *Plast Reconstr Surg* 2010;125(2):582–588.
10. Francesco G, Kolker D, Michael HR. Modified reverse sural artery flap with improved venous outflow in lower-leg reconstruction. *Ann Plast Surg* 2007;59(5):563–565.
11. Schlatterer D, Hirshorn K. Negative pressure wound therapy with reticulated open cell foam-adjunctive treatment in the management of traumatic wounds of the leg: A review of the literature. *J Orthop Trauma* 2008;22(10 Suppl):S152–160.
12. Chang SM, Hou CL. The development of the distally based radial forearm flap in hand reconstruction with preservation of the radial artery. *Plast Reconstr Surg* 2000;106(4):955–957.
13. Streubel PN, Stinner DJ, Obremskey WT. Use of negative-pressure wound therapy in orthopaedic trauma. *J Am Acad Orthop Surg* 2012;20(9):564–574.
14. Follmar KE, Baccarani A, Baumeister SP, Levin LS, Erdmann D. The distally based sural flap. *Plast Reconstr Surg* 2007;119(6):138e–148e.
15. Steinberger Z, Therattil PJ, Levin LS. Orthoplastic approach to lower extremity reconstruction: An update. *Clin Plast Surg* 2021;48(2):277–288.
16. McGregor IA, Morgan G. Axial and random pattern flaps. *Br J Plast Surg* 1973;26(3):202–213.
17. Bertelli JA. "Reply to Dr Mutaf." *Br J Plast Surg* 1994;47(2):143–144.
18. Cormack GC, Lamberty BG. A classification of fascio-cutaneous flaps according to their patterns of vascularisation. *Br J Plast Surg* 1984;37(1):80–87.
19. Masquelet AC, Romana MC, Wolf G. Skin island flaps supplied by the vascular axis of the sensitive superficial nerves: Anatomic study and clinical experience in the leg. *Plast Reconstr Surg* 1992;89(6):1115–1121.
20. Bertelli JA, Catarina S. Neurocutaneous island flaps in upper limb coverage: Experience with 44 clinical cases. *J Hand Surg Am* 1997;22(3):515–526.
21. Woodward KL, Kenshalo DR Sr. The recovery of sensory function following skin flaps in humans. *Plast Reconstr Surg* 1987;79(3):428–435.
22. Hermanson A, Dalsgaard CJ, Arnander C, Lindblom U. Sensibility and cutaneous reinnervation in free flaps. *Plast Reconstr Surg* 1987;79(3):422–427.
23. Potparic Z, Rajacic N. Long-term results of weight-bearing foot reconstruction with non-innervated and reinnervated free flaps. *Br J Plast Surg* 1997;50(3):176–181.
24. Pavletic MM, Watters J, Henry RW, Nafe LA. Reverse saphenous conduit flap in the dog. *J Am Vet Med Assoc* 1983;182(4):380–389.
25. Kostolich M, Pavletic MM. Axial pattern flap based on the genicular branch of the saphenous artery in the dog. *Vet Surg* 1987;16(3):217–222.
26. Miller JW. The Weigert-Pal technic for staining myelin. *Stain Technol*. 1926;1(2):72–73.
27. Bolton JS. On the nature of the Weigert-Pal method. *J Anat Physiol* 1898;32(Pt 2):247–266.
28. Garven HS, Gairns FW. The silver diammine ion staining of peripheral nerve elements and the interpretation of the results: With a modification of the Bielschowsky-Gros method for frozen sections. *Q J Exp Physiol Cogn Med Sci* 1952;37(3):131–142.